AIAA JOURNAL
Vol. 48, No. 11, November 2010

Analytical Solution of Converging Shock Wave in Magnetogasdynamics

L. P. Singh* and M. Singh†
Banaras Hindu University, Varanasi 221 005, India
and
Bishun D. Pandey‡
Ohio State University, Marion, Ohio 43302

DOI: 10.2514/1.J050244

In this paper, a similarity solution to a problem in magnetogasdynamics with strong converging cylindrical shock wave is examined. An analytical description of converging shock waves is presented by replacing the previous approach for numerical solutions of the ordinary differential equations with a theoretical study of the singular points of the differential equations. A study of singular points of the system of differential equations leads to an analytic description of the flowfield and a determination of the similarity exponent. The influences of adiabatic heat exponent and magnetic field strength on the flow pattern for various cases are assessed. The general behavior of the velocity and density distribution remains unaffected. However, the pressure profiles are greatly affected by the magnetic field interaction.

Nomenclature

a	=	sound speed
H	=	magnetic field strength
h	=	magnetic pressure
p	=	pressure of the gas
T	=	temperature
t	=	time
u	=	velocity
x	=	spatial coordinate
γ	=	specific heat ratio
μ	=	magnetic permeability
ρ	=	density of the gas
$\Re$	=	gas constant

I. Introduction

IN THE present paper we analyze the self-similar motion of converging cylindrical shock wave in ideal plasma of varying density. The plasma is assumed to be an ideal gas with an infinite electrical conductivity and permeated by an axial magnetic field orthogonal to the trajectories of gas particles. The medium is initially uniform and at rest. In the final stages of the collapse the shock becomes strong and the pressure ahead of the shock is neglected in comparison with the pressure behind the shock, leading to similarity formulation for the problem. The similarity variable, which is the ratio of distance to a particular power of the time, is not known a priori. Chisnell [1] has determined this particular power, known as similarity exponent, from the solution of a single ordinary differential equation. Many authors, e.g., Guderley [2], Butler [3], Sedov [4], Stanyukovich [5], Zeldovich and Raizer [6], Welsh [7], Lazarus [8], Hirschler and Gretler [9], Taylor and Cargill [10], Lock and Mestel [11], and Gurovich et al. [12] have described the methods for determination of the similarity exponent in uniform medium. Similarity exponent in non uniform medium has been determined by many researchers including Whitham [13], Hafner [14], Radha and Sharma [15], and Toque [16]. Gundersen [17] discussed the problem of cylindrical and spherical MHD shock waves and derived a relation between strengths of converging cylindrical and spherical magnetohydrodynamic shocks near the point of collapse and the distance from the point of collapse. Chisnell [1] provided an analytical description of converging shock waves by replacing the previous approach for numerical solutions of the ordinary differential equations with a theoretical study of the singular points of the differential equations. This theoretical approach leads to an approximate determination of the similarity exponent, which is in close agreement with previously obtained values. These extremely good, though approximate, values of the similarity exponent led to simple analytical description of the flowfield behind the converging shock waves.

In the present investigation, we determine the similarity exponent and an analytical description of the flowfield behind the converging shock wave in magnetogasdynamics. The study of singular points of the system of differential equations leads to an approximate determination of the similarity exponent and an analytical description of flowfield behind the shock wave. The influence of a change in the value of the adiabatic heat exponent γ and a change in the magnetic field strength on the flow pattern for various cases are assessed. The general behavior of the velocity and density distribution remains unaffected but the pressure profiles are greatly affected by the magnetic field interaction.

II. Basic Equations

Assuming the electrical conductivity to be infinite and the direction of the magnetic field to be orthogonal to the trajectories of the gas particles, the basic equations for a one-dimensional cylindrically symmetric motion in magnetogasdynamics can be written in the form [18]

$$\rho_t + u\rho_x + \rho u_x + \rho u x^{-1} = 0 \tag{1}$$

$$u_t + uu_x + \rho^{-1}(p_x + h_x) = 0 \tag{2}$$

$$p_t + up_x - a^2(\rho_t + u\rho_x) = 0 \tag{3}$$

$$h_t + uh_x + 2h(u_x + ux^{-1}) = 0 \tag{4}$$

Received 24 September 2009; revision received 3 August 2010; accepted for publication 6 August 2010.

*Department of Applied Mathematics, Institute of Technology; lpsingh.apm@itbhu.ac.in (Corresponding Author).
†Department of Applied Mathematics, Institute of Technology,
‡Department of Mathematics.

where ρ is the density, p the pressure, u the particle velocity; $a = (\gamma p/\rho)^{1/2}$ is the sound speed with γ as the constant specific heat ratio; $h = \mu H^2/2$ is the magnetic pressure with, H and μ being the magnetic field strength and the magnetic permeability, respectively; t is the time and x the single spatial coordinate. The letter subscripts denote partial differentiation unless stated otherwise. The system of Eqs. (1–4) is supplemented with an equation of state $p = \rho\Re T$, in which $\Re$ is the gas constant and T is the temperature.

III. Similarity Transformations

We introduce the nondimensional variables G, V, Z, and B so that the flow variables are written with these new variables in the following form

$$\rho = \rho_0 G, \qquad u = \frac{x}{t}V, \qquad a^2 = \frac{x^2}{t^2}Z, \qquad b^2 = \frac{x^2}{t^2}B \tag{5}$$

where $b = (2h/\rho)^{1/2}$ is the Alfvén speed.

The motion of the shock takes place for $t < 0$, arriving at the origin O at time $t = 0$. The Eqs. (1–4) in terms of new nondimensional variables G, V, Z, and B reduces to the following form

$$tG_t + xVG_x + xGV_x = -2VG \tag{6}$$

$$tV_t + xVV_x + \frac{xZ_x}{\gamma} + \frac{xZG_x}{\gamma G} + \frac{xB_x}{2} + \frac{xBG_x}{2G} = V - V^2 - \frac{2Z}{\gamma} - B \tag{7}$$

$$\frac{tZ_t}{Z} + \frac{xVZ_x}{Z} - \frac{(\gamma-1)}{G}(tG_t + xVG_x) = 2 - 2V \tag{8}$$

$$\frac{tB_t}{B} + \frac{tG_t}{G} + \frac{xVB_x}{B} + \frac{xVG_x}{G} + 2xV_x = 2 - 6V \tag{9}$$

Self-similar solutions of Eqs. (6–9) are sought in terms of the variable $\xi = x/R(t)$, where $R(t)$ is the distance of the shock from the origin at time $t\,(<0)$ and G, V, Z, and B are functions of ξ alone. Changing the independent variables from (x, t) to (ξ, t) using

$$\frac{\partial}{\partial x} = \frac{1}{R}\frac{\partial}{\partial \xi}, \qquad \frac{\partial}{\partial t} = \frac{\partial}{\partial t} - \xi\frac{\dot{R}}{R}\frac{\partial}{\partial \xi} \tag{10}$$

where $\dot{R} = \frac{dR}{dt}$.

It is noted from Eqs. (6–9) that the t- variable enters the equations only in the combination $t\dot{R}/R$ arising from the $t\partial/\partial t$ term. Thus, the condition for the self-similar solution to exist is

$$t\dot{R}/R = \alpha \quad \text{or} \quad R = A(-t)^{\alpha} \tag{11}$$

where α and A are constants. The Eqs. (6–9) in terms of $V(\xi)$, $G(\xi)$, $Z(\xi)$, and $B(\xi)$ reduces to

$$\xi V' + (V-\alpha)\xi\frac{G'}{G} = -2V \tag{12}$$

$$(V-\alpha)\xi V' + \left(\frac{Z}{\gamma} + \frac{B}{2}\right)\xi\frac{G'}{G} + \xi\frac{Z'}{\gamma} + \xi\frac{B'}{2} = V - V^2 - \frac{2Z}{\gamma} - B \tag{13}$$

$$(\gamma-1)Z\xi\frac{G'}{G} - \xi Z' = \frac{-2Z(1-V)}{V-\alpha} \tag{14}$$

$$2B\xi V' + (V-\alpha)B\xi\frac{G'}{G} + (V-\alpha)\xi B' = (2-6V)B \tag{15}$$

The system of Eqs. (12–15) can be solved for the derivatives V', G', Z', and B' in the following form:

$$\xi V' = \frac{\Delta_1}{\Delta}, \qquad \frac{\xi G'}{G} = \frac{\Delta_2}{\Delta}, \qquad \xi Z' = \frac{\Delta_3}{\Delta}, \qquad \xi B' = \frac{\Delta_4}{\Delta} \tag{16}$$

where

$$\Delta = -Z - B + (V-\alpha)^2 \tag{17}$$

is the determinant of the left-hand side coefficients and Δ_i, $i = 1, 2, 3, 4$ are the determinants obtained by replacing the ith column of Δ by the right-hand side of Eqs. (12–15). The four determinants Δ_i are given by

$$\Delta_1 = -\Delta\left(2V - \frac{2(1-\alpha)}{\gamma}\right) - (\alpha - V)Q(V) + B(1-\alpha)\left(\frac{2}{\gamma} - 1\right) \tag{18}$$

$$\Delta_2 = \frac{2\Delta(1-\alpha)}{\gamma(\alpha - V)} - Q(V) + \frac{B}{(\alpha - V)}(1-\alpha)\left(\frac{2}{\gamma} - 1\right) \tag{19}$$

$$\Delta_3 = \frac{Z}{V-\alpha}\left[2\Delta\left(\alpha - V + \frac{1-\alpha}{\gamma}\right) + (\gamma-1)(\alpha - V)Q(V) - (\gamma-1)B(1-\alpha)\left(\frac{2}{\gamma} - 1\right)\right] \tag{20}$$

$$\Delta_4 = \frac{B}{V-\alpha}\left[2\Delta\left(1 - V - \left(\frac{1-\alpha}{\gamma}\right)\right) + (\alpha - V)Q(V) - B(1-\alpha)\left(\frac{2}{\gamma} - 1\right)\right] \tag{21}$$

where

$$Q(V) = V^2 + \left(1 - 2\alpha - \frac{2(1-\alpha)}{\gamma}\right)V + \frac{2\alpha(1-\alpha)}{\gamma} \tag{22}$$

In Eq. (16) ξ occurs as the coefficients of its derivatives, and G does not occur in the determinants, the system of equations could be decoupled to provide a pair of ordinary differential equations

$$\frac{dZ}{dV} = \frac{\Delta_3}{\Delta_1} \tag{23}$$

$$\frac{dB}{dV} = \frac{\Delta_4}{\Delta_1} \tag{24}$$

with two supplementary equations

$$\frac{1}{G}\frac{dG}{dV} = \frac{\Delta_2}{\Delta_1} \tag{25}$$

$$\frac{1}{\xi}\frac{d\xi}{dV} = \frac{\Delta}{\Delta_1} \tag{26}$$

The system Eqs. (23–26) can be solved after determining $Z(V)$ and $B(V)$ from Eqs. (23–26), respectively. To describe the flow behind the shock, a solution of the Eq. (16) is required which, at the shock $\xi = 1$, satisfies the Rankine–Hugoniot conditions for a strong shock

$$\rho = \frac{\gamma+1}{\gamma-1}\rho_0, \qquad u = \frac{2}{\gamma+1}\dot{R}$$
$$a^2 = \frac{2\gamma(\gamma-1)}{(\gamma+1)^2}\dot{R}^2, \qquad b^2 = \left(\frac{\gamma+1}{\gamma-1}\right)^2\dot{R}^2 \tag{27}$$

Using Eq. (11) in Eq. (5), the flow variable may be written as in the terms of ξ, t as following

$$\left.\begin{aligned} \rho = \rho_0 G, \qquad u = \tfrac{\dot R}{\alpha}\xi V, \qquad p = \tfrac{\rho_0 \dot R^2}{\gamma\alpha^2}\xi^2 GZ, \\ h = \tfrac{\rho_0 \dot R^2}{\gamma\alpha^2}\xi^2 GB, \quad a^2 = \tfrac{\dot R^2}{\alpha^2}\xi^2 Z, \qquad b^2 = \tfrac{\dot R^2}{\alpha^2}\xi^2 B \end{aligned}\right\} \tag{28}$$

The transformed boundary conditions at the shock ($\xi = 1$) become

$$G_s = \frac{\gamma+1}{\gamma-1}, \qquad V_s = \frac{2\alpha}{\gamma+1}$$
$$Z_s = \frac{2\gamma(\gamma-1)}{(\gamma+1)^2}\alpha^2, \qquad B_s = \left(\frac{\gamma+1}{\gamma-1}\right)^2\alpha^2 \tag{29}$$

behind the shock, where x is large, Eq. (5) shows that

$$V(\infty) = 0, \qquad Z(\infty) = 0, \qquad B(\infty) = 0 \tag{30}$$

It may be noted that $\Delta = 0$ is a parabola in the (V, Z) plane touching the V axis at $V = \alpha$. Equation (28) shows that Δ has a negative value at the shock $\xi = 1$ and a positive value at $\xi = \infty$. Thus, the solution curve has to cross the parabola to reach the origin represent the condition behind the shock. The solution curve and the parabola $\Delta = 0$ are shown in Fig. 1 for cylindrical shock with $\gamma = 1.4$. Equation (16) show that at a point on the parabola $\Delta = 0$, the flow variables will have infinite slopes unless Δ_i simultaneously vanishes. To get the nonsingular solution of Eq. (16), we choose the exponent α in such way that Δ vanishes at those points where the determinant Δ_i vanishes. Here we use the numerical determination method for the similarity exponent given by Chisnell [1] and formulated by Zeldovich and Raizer [6].

IV. Determination of the Similarity Exponent

In this section the behavior of the differential equations that determines the similarity exponent is examined at two singular points. Using Eqs. (18–21), the Eqs. (23) and (24) may be written as

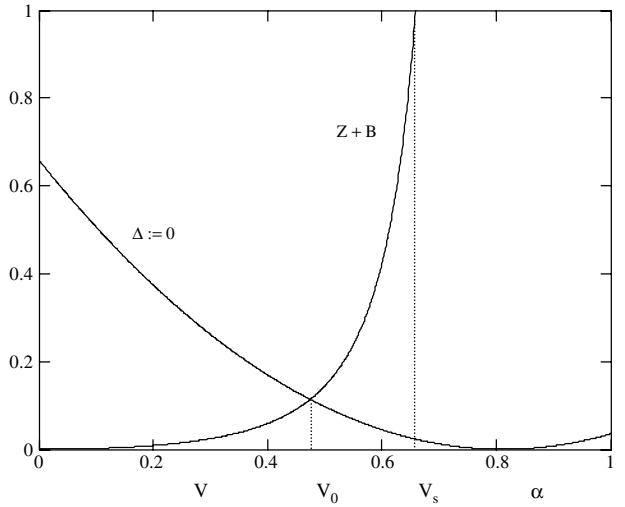

Fig. 1 The solution curve ($Z + B$) and the parabola $\Delta = 0$ for $\gamma = 1.4$. The solution curve has a singular point at V_0, the shock at V_s, and the origin corresponds to conditions far behind the shock.

$$Q = (V - V_0)\left(V - \frac{2\alpha(1-\alpha)}{\gamma V_0}\right) \tag{35}$$

Using above values of Δ and Q, Eqs. (31) and (32) reduces in the following form

$$\frac{1}{Z}\frac{\mathrm{d}Z}{\mathrm{d}V} = \frac{N_1}{V} + \frac{N_2}{\alpha - V} + \frac{N_3}{V+q} \tag{36}$$

where

$$\frac{1}{Z}\frac{\mathrm{d}Z}{\mathrm{d}V} = \frac{2\Delta(\alpha - V + \frac{1-\alpha}{\gamma}) + (\gamma-1)(\alpha-V)Q(V) - (\gamma-1)B(1-\alpha)(\frac{2}{\gamma}-1)}{2\Delta(V - \frac{1-\alpha}{\gamma})(\alpha-V) + (\alpha-V)^2 Q(V) - (\alpha-V)B(1-\alpha)(\frac{2}{\gamma}-1)} \tag{31}$$

$$\frac{1}{B}\frac{\mathrm{d}B}{\mathrm{d}V} = \frac{2\Delta(1 - V - \frac{1-\alpha}{\gamma}) + (\alpha-V)Q(V) - B(1-\alpha)(\frac{2}{\gamma}-1)}{2\Delta(V - \frac{1-\alpha}{\gamma})(\alpha-V) + (\alpha-V)^2 Q(V) - (\alpha-V)B(1-\alpha)(\frac{2}{\gamma}-1)} \tag{32}$$

By taking note of the correct behavior of Z and B at the singular points, two trial functions Z_T and B_T are constructed which, when substituted into Δ in right-hand side of Eqs. (31) and (32) leads to extremely accurate values of the similarity exponent α and a simple analytic description of the flowfield. The integration of Eqs. (31) and (32) has to be performed without knowing a priori, the value of V at which the solution crosses the parabola $\Delta = 0$. If this value is $V = V_0$, then $Q(V_0) = 0$ and $Z_T(V_0) + B_T(V_0)$ must equal $(\alpha - V_0)^2$. We introduce the trial function developed by Chisnell [1]

$$Z_T = k\lambda V^2 \quad \text{and} \quad B_T = (1-k)\lambda V^2 \tag{33}$$

where $\lambda = (\frac{\alpha}{V_0} - 1)^2$ and $0 < k < 1$ has required value at V_0 is finite at $V = \alpha$.

Inserting the trial functions into Δ in the right-hand side of Eqs. (31) and (32) enables the singular behavior at $V = V_0$ be removed as both Δ and Q will have the factor $V - V_0$. On using Eq. (33), expressions for Δ and Q reduces to

$$\Delta = (V - V_0)\left(V(1-\lambda) - \frac{\alpha^2}{V_0}\right) \tag{34}$$

$$q = \frac{1}{1-2\lambda}\left[\alpha + (1-\alpha)\left\{\lambda(1-k) - \frac{2}{\gamma}(1-\lambda k) + \frac{2\alpha}{\gamma V_0}\right\} - \frac{2\alpha^2}{V_0}\right]$$
$$N_1 = -\frac{2\alpha}{qV_0(1-2\lambda)}$$
$$N_2 = \frac{1}{(\alpha+q)(1-2\lambda)}\left[K - (1-2\lambda+\gamma)\alpha - \frac{2\alpha}{V_0}\right]$$
$$N_3 = \frac{1}{(\alpha+q)(1-2\lambda)}\left[(1-\alpha)(1-2\lambda+\gamma) + K + \frac{2\alpha^2}{qV_0}\right]$$
$$K = \alpha\left(\gamma + 3 + \frac{2\alpha}{V_0}\right) + \lambda(1-k)(\gamma - 3 - \alpha) + \frac{2(1-\alpha)}{\gamma}\left(1 - k\lambda - \frac{\alpha}{V_0}\right)$$
$$\frac{1}{B}\frac{\mathrm{d}B}{\mathrm{d}V} = \frac{N_1}{V} + \frac{K_1}{\alpha - V} + \frac{K_2}{V+q} \tag{37}$$

where

$$K_1 = \frac{1}{(\alpha+q)(1-2\lambda)}\left[K^* - \alpha(3-2\lambda) - \frac{2\alpha}{V_0}\right]$$

$$K_2 = \frac{1}{(\alpha+q)(1-2\lambda)}\left[K^* + q(3-2\lambda) - \frac{2\alpha^2}{qV_0}\right]$$

$$K^* = 2 + \alpha\left(1 - \frac{2\alpha}{V_0}\right) + \frac{2(1-\alpha)}{\gamma}\left(\frac{\alpha}{V_0} - 1\right) + \lambda\left[k(1-\alpha)\left(\frac{1}{\gamma} - 1\right) + \frac{k}{\gamma} - 1 - \alpha\right]$$

To determine α by a simple iteration scheme a solution of the system of simultaneous Eqs. (36) and (37) is required and it must pass through points (V_0, Z_0), (V_0, B_0) and the shock points (V_s, Z_s), (V_s, B_s). Integration from V_0 to V_s gives

$$\frac{Z_s}{Z_0} = \left(\frac{V_s}{V_0}\right)^{N_1}\left(\frac{\alpha - V_0}{\alpha - V_s}\right)^{N_2}\left(\frac{V_s+q}{V_0+q}\right)^{N_3} \tag{38}$$

$$\frac{B_s}{B_0} = \left(\frac{V_s}{V_0}\right)^{N_1}\left(\frac{\alpha - V_0}{\alpha - V_s}\right)^{K_1}\left(\frac{V_s+q}{V_0+q}\right)^{K_2} \tag{39}$$

as the condition to be satisfied by the parameters α and V_0. Substituting V_s, Z_s and B_s from Eq. (29) in Eqs. (38) and (39), $Z_0 = k(\alpha - V_0)^2$ and $B_0 = (1-k)(\alpha - V_0)^2$ provides

$$\left(\frac{\alpha}{V_0} - 1\right)^2 = \left(\frac{\gamma+1}{2}\right)^{N_1}\left(\frac{V_0}{\alpha}\right)^{N_1-2} \times \left\{\frac{2\gamma(\gamma-1)}{(\gamma+1)^2}\left(\frac{\gamma-1}{(\gamma+1)(1-\frac{V_0}{\alpha})}\right)^{N_2}\left(\frac{V_0+q}{\frac{2\alpha}{\gamma+1}+q}\right)^{N_3}\right\} + \left(\frac{\gamma+1}{2}\right)^{N_1}\left(\frac{V_0}{\alpha}\right)^{N_1-2}\left\{\left(\frac{\gamma+1}{\gamma-1}\right)^2 \times \left(\frac{\gamma-1}{(\gamma+1)(1-\frac{V_0}{\alpha})}\right)^{K_1}\left(\frac{V_0+q}{\frac{2\alpha}{\gamma+1}+q}\right)^{K_2}\right\} \tag{40}$$

The relation between α and V_0 is given by the condition $Q(V_0) = 0$ and Q is given by Eq. (22).

By rearranging the terms in Eq. (22), V_0 may be written in terms of α as

$$\frac{\alpha}{1-\alpha} = \frac{1}{1 - V_0/\alpha} + \frac{2}{\gamma V_0/\alpha} \tag{41}$$

This explicit determination of $\alpha/(1-\alpha)$ in terms of V_0/α can be used as the iteration parameter in the solution of Eq. (40). For a given V_0/α, having determined $\alpha/(1-\alpha)$, the parameter α and V_0 follow and may be inserted in the right side of Eq. (40). Substituting $N_1 = 2$, $N_2 = 0$, $N_3 = 0$, $K_1 = 0$, and $K_2 = 0$ in Eq. (40), we achieve a good initial approximation of α/V_0. The results for the similarity exponent α for various values of γ and k are given in Table 1.

It can be seen from fore going analysis that as γ increases from unity, the value of $\alpha/(1-\alpha)$ and α decreases and the two zeros of quadratic expression $Q(V)$ move closer to each other. Writing Eq. (22) in the form

$$\frac{Q(V)}{\alpha^2} = \left(\frac{V}{\alpha} - \frac{1}{2}\left(1 + \frac{1}{\beta}\left(\frac{2}{\gamma} - 1\right)\right)\right)^2 - \frac{1}{4\beta^2}\left(\left(\beta - \left(\frac{2}{\gamma} + 1\right)\right)^2 - \frac{8}{\gamma}\right) \tag{42}$$

where

$$\beta = \alpha/(1-\alpha) \tag{43}$$

It may be noted that the roots of $Q(V)$ will coincide if

$$\beta = \{1 + (2/\gamma)^{1/2}\}^2 \tag{44}$$

and this particular location of singular point V_0 may be written as

$$\frac{\alpha}{V_0} = 1 + (\gamma/2)^{1/2} \tag{45}$$

It is evident from Eqs. (44) and (45) that as γ increases, the value of α/V_0 increases and the value of β decreases.

V. Flowfield

In the previous section, the similarity exponent α was determined for various values of γ and k by solving differential equations for V, Z and V, B, which passed through the singular point V_0, Z_0, B_0, and V_s, Z_s, B_s. Now the supplementary differential equations for G and ξ in Eqs. (25) and (26) are integrated. These equations also have a singular point at V_0. The trial function $Z_T + B_T$ given in Eq. (33) is used to remove the factor $(V - V_0)$ from the numerators and denominators of the right-hand side of Eqs. (25) and (26). Appropriate expansions of Δ and Q are given in Eqs. (34) and (35), respectively, and the corresponding expansions for Δ_1 and Δ_2 given by Eqs. (18) and (19) are

$$\Delta_1 = -(V - V_0)V(1-\lambda)(V+q) \tag{46}$$

$$\Delta_2 = (V - V_0)\left\{\left(V(1-\lambda) - \frac{\alpha^2}{V_0}\right)(1-\alpha) - (\alpha - V)\mathrm{x}\left(V - \frac{2\alpha(1-\alpha)}{\gamma V_0}\right) + \left(V(1-k\lambda) - \frac{\alpha^2}{V_0}\right)(1-\alpha)\left(\frac{2}{\gamma} - 1\right)\right\} \tag{47}$$

Substituting the values of Δ, Q, Δ_1 and Δ_2 in Eqs. (25) and (26) yields

$$\frac{1}{G}\frac{\mathrm{d}G}{\mathrm{d}V} = \frac{L_1}{V - \alpha} + \frac{L_2}{V+q} \tag{48}$$

$$\frac{1}{\xi}\frac{\mathrm{d}\xi}{\mathrm{d}V} = \frac{-\alpha N_1}{2V} + \frac{L_3}{V+q} \tag{49}$$

where

$$L_1 = \frac{\alpha + q_1}{(\alpha+q)(1-2\lambda)}, \qquad L_2 = \frac{q - q_1}{(\alpha+q)(1-2\lambda)}$$

$$L_3 = \frac{\alpha N_1}{2} + \frac{\lambda - 1}{1 - 2\lambda}$$

$$q_1 = 1 + (1-\alpha)\left\{\left(\frac{2}{\gamma} - 1\right)(1 - k\lambda) - 1\right\} - 2\alpha\left(1 + \frac{\alpha}{\gamma V_0}\right)$$

Integration of Eqs. (36), (37), (48), and (49) from the shock $\xi = 1$ provides:

$$\frac{Z}{Z_s} = \left(\frac{V}{V_s}\right)^{N_1}\left(\frac{\alpha - V_s}{\alpha - V}\right)^{N_2}\left(\frac{V+q}{V_s+q}\right)^{N_3} \tag{50}$$

$$\frac{B}{B_s} = \left(\frac{V}{V_s}\right)^{N_1}\left(\frac{\alpha - V_s}{\alpha - V}\right)^{K_1}\left(\frac{V+q}{V_s+q}\right)^{K_2} \tag{51}$$

$$\frac{G}{G_s} = \left(\frac{\alpha - V}{\alpha - V_s}\right)^{L_1}\left(\frac{V+q}{V_s+q}\right)^{L_2} \tag{52}$$

$$\xi = \left(\frac{V_s}{V}\right)^{\frac{\alpha N_1}{2}}\left(\frac{V+q}{V_s+q}\right)^{L_3} \tag{53}$$

with V_s, Z_s, B_s, and G_s given in Eq. (29). Using Eqs. (28) and (29) the nondimensional form of flow variables are written as

$$\frac{u}{u_s} = \xi\frac{V}{V_s} = \left(\frac{V}{V_s}\right)^{(1-\frac{\alpha N_1}{2})}\left(\frac{V+q}{V_s+q}\right)^{L_3} \tag{54}$$

$$\frac{\rho}{\rho_s} = \frac{G}{G_s} = \left(\frac{\alpha - V}{\alpha - V_s}\right)^{L_1}\left(\frac{V+q}{V_s+q}\right)^{L_2} \tag{55}$$

$$\frac{p}{p_S} = \xi^2 \frac{G}{G_s}\frac{Z}{Z_s} = \left(\frac{V}{V_s}\right)^{(1-\alpha)N_1}\left(\frac{\alpha - V}{\alpha - V_s}\right)^{L_1 - N_2}\left(\frac{V+q}{V_s+q}\right)^{N_2+L_2+2L_3} \tag{56}$$

$$\frac{h}{h_s} = \xi^2 \frac{G}{G_s}\frac{B}{B_s} = \left(\frac{V}{V_s}\right)^{(1-\alpha)N_1}\left(\frac{\alpha - V}{\alpha - V_s}\right)^{L_1 - K_1}\left(\frac{V+q}{V_s+q}\right)^{K_2+L_2+2L_3} \tag{57}$$

VI. Results and Discussion

The inverse density, the gas velocity, the pressure, and the magnetic pressure normalized with respect to its value at the shock are computed using Eqs. (54–57) for different values of k and specific heat ratio γ. The flow and field profiles are presented in Figs. 2–5. It may be noted here that the magnetic pressure term enters into the solution through trial functions defined in Eq. (33) with $0 < k \leq 1$. For $k = 1$, the analysis reduces to the case described by Chisnell [1]. Smaller values of k signify the higher magnetic field effect. The value α corresponding to different values of the specific heat ratio γ and k are given in Table 1. The fact that α is always less than one shows that the shock wave is continuously accelerated. The computed results indicate that an increase in the specific heat ratio γ or k causes the similarity exponent α to decrease. In fact, the presence of the magnetic field ahead of the shock has an important effect on the flowfield behind the shock.

Numerical computation of Eqs. (54–57) for $1 < \xi \leq \infty$ has been performed in terms of a new variable $y = 1/\xi$, and the range of computation is $0 < y < 1$. In Figs. 2–5, : kWe find that the density increases monotonically behind the shock and has a nonzero limiting value far behind the shock. The inverse density variable, ρ_s/ρ as a function of $1/\xi$, is displayed Fig. 2 for cylindrical shocks with various values of γ and k. Also, an increase in γ and magnetic field strength causes ρ_s/ρ to increase. The monotonic decreasing variable u/u_s is displayed as a function of $1/\xi$, using Eq. (54) in Fig. 3 for cylindrical shocks for various value of γ and k. The effect of

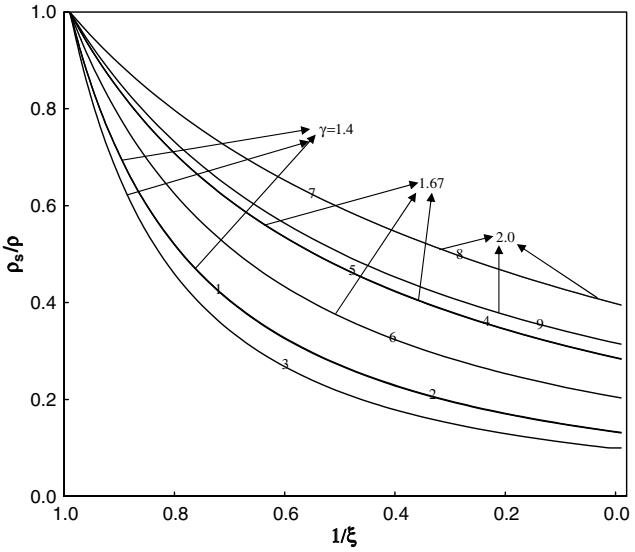

Fig. 2 The inverse density, normalized with respect to its values at shock, is shown as function $1/\xi$ for various values γ and k. The numbers on the lines correspond to the following different values of k: 1) 0.4, 2) 0.5, 3) 0.6, 4) 0.4, 5) 0.5, 6) 0.6, 7) 0.4, 8) 0.5, and 9) 0.6.

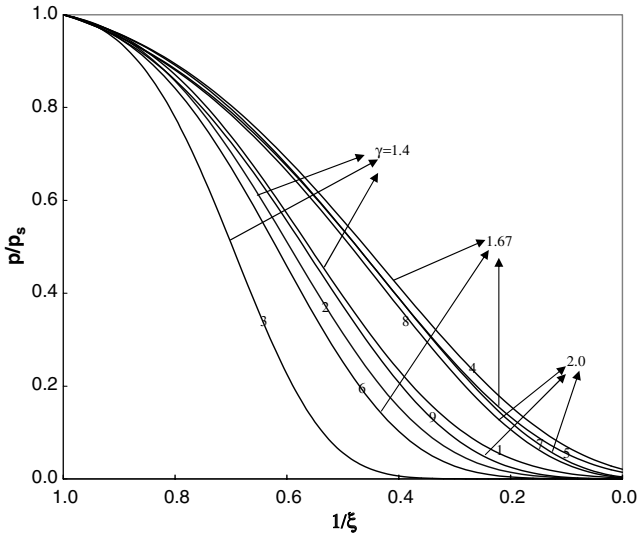

Fig. 4 The pressure, normalized with respect to its values at shock, is shown as function $1/\xi$ for various values γ and k. The numbers on the lines correspond to the following different values of k: 1) 0.4, 2) 0.5, 3) 0.6, 4) 0.4, 5) 0.5, 6) 0.6, 7) 0.4, 8) 0.5, and 9) 0.6.

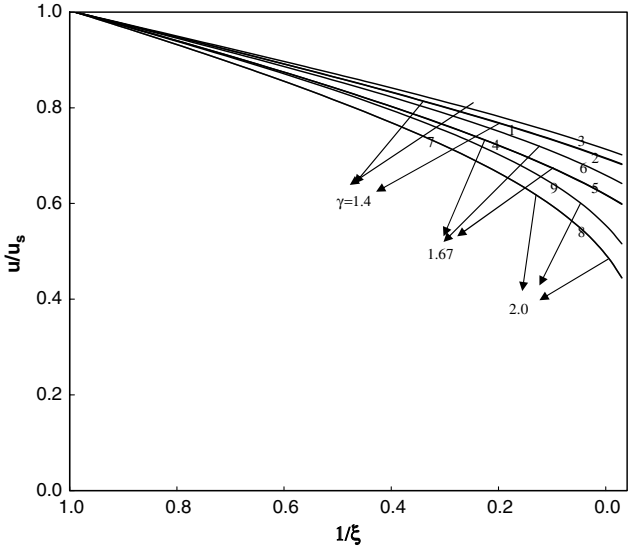

Fig. 3 The fluid velocity, normalized with respect to its values at shock, is shown as function $1/\xi$ for various values γ and k. The numbers on the lines correspond to the following different values of k: 1) 0.4, 2) 0.5, 3) 0.6, 4) 0.4, 5) 0.5, 6) 0.6, 7) 0.4, 8) 0.5, and 9) 0.6.

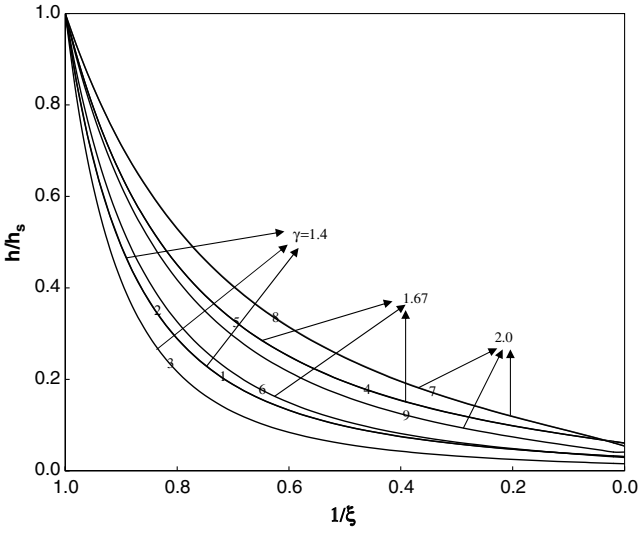

Fig. 5 The magnetic pressure, normalized with respect to its values at shock, is shown as function $1/\xi$ for various values γ and k. The numbers on the lines correspond to the following different values of k: 1) 0.4, 2) 0.5, 3) 0.6, 4) 0.4, 5) 0.5, 6) 0.6, 7) 0.4, 8) 0.5, and 9) 0.6.

Table 1 The values of α and α/V_0 obtained from Eqs. (40) and (41) for various values of γ and k

γ	k	α	α/V_0
1.3	0.1	.841327	1.502220
	0.4	.841304	1.502597
	0.5	.841281	1.503468
	0.6	.841251	1.503468
	0.9	.841105	1.505884
1.4	0.1	.830089	1.660501
	0.4	.830132	1.659623
	0.5	.830132	1.65962
	0.6	.830128	1.659776
	0.9	.830089	1.661314
1.67	0.1	.814361	1.894759
	0.4	.814358	1.894759
	0.5	.814357	1.897624
	0.6	.814356	1.897624
	0.9	.814352	1.900930
2.0	0.1	.800111	2.054208
	0.4	.800128	2.058177
	0.5	.800135	2.059650
	0.6	.800141	2.061204
	0.9	.800165	2.066400

increasing values of γ and magnetic field strength (lower values of k) causes u/u_s to decrease. The pressure distribution p/p_s is displayed using Eq. (56) in Fig. 4 for cylindrical shocks for various values of γ and k. The behavior of the gas pressure in the magnetogasdynamics case is in contrast to the corresponding nonmagnetic case. The monotonic decreasing behavior of pressure is displayed as a function of $1/\xi$ for different values of γ and k in Fig. 4. It is clear from the figure that an increase in magnetic pressure causes to slow down the process of steepening compared with lower magnetic pressure levels and nonmagnetic case (Chisnell [1]) for all values of γ. This shows that an increase of the magnetic field strength has just the reverse effect in the sense that it effectively resists the compression. Also an increase in the value of γ causes a falling off of the pressure levels. The magnetic pressure profiles as a function of $1/\xi$ are displayed using Eq. (57) in Fig. 5 for various values of γ and magnetic field strength. The effect of increasing values of γ and magnetic field strength is to increase the magnetic pressure levels in the flowfield.

VII. Conclusions

The self-similar motion of converging cylindrical shock waves in ideal plasma with varying density has been analyzed. The plasma is considered to have infinite electrical conductivity and to be permeated by an axial magnetic field orthogonal to the trajectories of gas particles. Using the method developed by Chisnell [1] the similarity exponent has been determined and an analytical description of the flowfield behind the shock has been presented. It has been observed that as the magnetic field strength decreases the value of the similarity exponent decreases. Also, the density distribution, velocity distribution, pressure distribution, and magnetic pressure profiles are presented for various values of the specific heat ratio γ and k. It has been observed that the density and velocity distribution profiles have similar behavior as in nonmagnetic case. However, the pressure profiles are greatly affected by the magnetic field.

Acknowledgment

Financial support from Institute of Technology, Banaras Hindu University in Varanasi, India is gratefully acknowledged.

References

[1] Chisnell, R. F., "An Analytic Description of Converging Shock Waves," *Journal of Fluid Mechanics*, Vol. 354, Jan. 1998, pp. 357–375. doi:10.1017/S0022112097007775

[2] Guderley, G., "Starke Kugelige und Zylindrische, Verdichtungsstosse in Der Nahe Des Kugelmitteelpunktes bzw der Zylinderachse," *Luftfahrtforschung*, Vol. 19, 1942, pp. 302–312.

[3] Butler, D., "Converging Spherical and Cylindrical Shocks," Ministry of Supply, Armament Research Establishment, United Kingdom, Rept. 54/54, 1954.

[4] Sedov, L. I., *Similarity and Dimensional Methods in Mechanics*, Academic Press, Newyork, 1959.

[5] Stanyukovich, K. P., *Unsteady Motion of Continuous Media*, Pergamon Press, New York, 1960.

[6] Zeldovich, Y. B., and Raizer, Y. P., *Physics of Shock Waves and High Temperature Hydrodynamic Phenomenon*, Vol. 2, Academic Press, New York, 1967.

[7] Welsh, R. L., "Imploding Shocks and Detonations," *Journal of Fluid Mechanics*, Vol. 29, No. 1, 1967, pp. 61–79. doi:10.1017/S0022112067000631

[8] Lazarus, R. B., "Self-Similar Solutions for Converging Shocks and Collapsing Cavities," *SIAM Journal on Numerical Analysis*, Vol. 18, No. 2, 1981, pp. 316–371. doi:10.1137/0718022

[9] Hirschler, T., and Gretler, W., "On the Eigenvalue Problem of Imploding Shock Waves," *Zeitschrift fur Angewandte Mathematik und Physik*, Vol. 52, No. 1, 2001, pp. 151–166. doi:10.1007/PL00001537

[10] Taylor, M. G. G. T., and Cargill, P. J., "A General Theory of Self-similar Expansion Waves in Magnetohydrodynamic flows," *Journal of Plasma Physics*, Vol. 66, No. 4, 2001, pp. 239–257. doi:10.1017/S0022377801001398

[11] Lock, R. M., and Mestel, A. J., "Annular Self-similar Solutions in Ideal Magnetogasdynamics," *Journal of Plasma Physics*, Vol. 74, No. 4, 2008, pp. 531–554. doi:10.1017/S0022377808007101

[12] Gurovich, V., Grinenko, A., and Krasik, Y., "Semianalytical Solution of the Problem of Converging Shock Waves," *Physical Review Letters*, Vol. 99, 2007, pp. 124503(1)–124503(4).

[13] Whitham, G. B., *Linear and Nonlinear Waves*, Interscience Publishers, New York, 1974.

[14] Hafner, P., "Strong Convergent Shock Waves Near the Centre of Convergence: A Power Series Solution," *SIAM Journal on Applied Mathematics*, Vol. 48, No. 6, 1988, pp. 1244–1261. doi:10.1137/0148076

[15] Radha, C., and Sharma, V. D., "Imploding Cylindrical Shock in a Perfectly Conducting and Radiating Gas," *Physics of Fluids B*, Vol. 5, No. 12, 1993, pp. 4287–4294. doi:10.1063/1.860596

[16] Toque, N., "Self Similar Implosion of a Continuous Stratified Medium," *Shock Waves*, Vol. 11, No. 3, 2001, pp. 157–165. doi:10.1007/PL00004074

[17] Gundersen, Roy M., "Cylindrical and Spherical Shock Waves in Monatomic Conducting Fluids," *Applied Scientific Research*, Section B Vol. 10, No. 2, 1963, pp. 119–128.

[18] Korobeinikov, V. P., *Problem in the Theory of Point Explosion in Gases*, American Mathematical Society, Providence, RI, 1970.

X. Zhong
Associate Editor